

# Comparative Evaluation of DTC Strategies for the Synchronous Reluctance Machine

Simon Wiedemann

MACCON GmbH

Aschauer-Str. 21

81549 Munich, Germany

Email: s.wiedemann@maccon.de

Arkadiusz Dziechciarz

Technical University of Cluj-Napoca

28 Memorandumului

Cluj-Napoca, Romania

Email: arkadiusz.dziechciarz@mae.utcluj.ro

**Abstract**—This paper evaluates the performance of the Direct Torque Control (DTC) and Direct Torque Control - Space Vector Modulation (DTC-SVM) for the Synchronous Reluctance Motor (SynRM). Both methods are compared to Field Oriented Control (FOC) with respect to output torque ripple, phase current - total harmonic distortion (THD) and electromagnetic torque dynamics of the motor based on simulations in Matlab/Simulink.

**Keywords**—Synchronous Reluctance Machine, Direct Torque Control, Space Vector Modulation, Torque Ripple, Total Harmonic Distortion.

## I. INTRODUCTION

The demand for permanent magnet free AC drives, less torque and current distortion, and high efficiency per volume are some of the reasons why the synchronous reluctance machine (SynRM) is considered as an alternative to widespread electric drives such as the Permanent Magnet Synchronous Machine (PMSM), Induction Machine (IM) and the Switched Reluctance Machine (SRM) [12], [13], [15], [19], [20], [21]. Field Oriented Control (FOC) and Direct Torque Control (DTC) are standard control methods in high performance electrical drive applications and their performance is commonly improved by introducing Space Vector Modulation (SVM). Advantages of SVM are the minimization of phase current harmonics, reduction of output torque ripple, constant switching frequency and the extension of the effective DC supply voltage of the Voltage Source Inverter (VSI) [2], [8], [18]. DTC enables fast reference torque tracking at load disturbances but results usually in variable switching frequency and higher output torque ripple in comparison with FOC. The DTC method will be also applicable if the number of Proportional-Integral (PI) controllers shall be reduced. Additionally, the computational effort of the general DTC scheme is minimized compared to FOC through the absence of computationally heavy

frame transformations [5]. Through the widespread use of DTC and DTC-SVM in PMSM and IM drive control it is necessary to review their performance for the SynRM with regard to output torque ripple, phase current distortion, switching frequency and torque dynamic.

The general DTC scheme of the SynRM is presented in [16] on which the following work is oriented. Reference [13] carried out a theoretical performance analysis for several current angles of the SynRM including Maximum Power Factor Control (MPFC) which is also applied within this paper. The author in [8] proposes a mixed control architecture consisting of the general DTC and the DTC-SVM for the induction motor and in [18] for the SynRM (RSM). Within this control architecture the DTC applies as long as the torque and flux errors are large. In case of small errors the DTC-SVM strategy applies. This enables fast reference torque tracking at load torque disturbances and reduced output current and torque distortion in steady state condition. However, the DTC-SVM method in [8], [18] requires an accurate measurement of the rotor position in order to perform the frame transformation which can be seen as a drawback for some applications. Furthermore, the author derives the reference direct- and quadrature axis voltage components from the outputs of two PI controllers which results in two additional controllers in addition to the speed PI controller. In contrast to [8], [18] the author of [1] performs the DTC-SVM for the PMSM directly in the stator reference frame which does not require an exact determination of the rotor position. The author proposes a technique in which the voltage references can be derived from a prediction of the stator flux-linkage in consideration of a flux-linkage displacement angle. This approach consists of a total number of two PI controllers which is one of the reasons for its employed within this work. A comparative performance study between FOC and DTC for PMSM is presented in [7] and for the IM in

[5]. A comparison of different DTC control architectures for the PMSM is presented in [6], [17]. In order to give a comparison between these methods for the SynRM this work presents a performance evaluation of DTC and DTC-SVM with respect to the performance of the FOC.

The following sections include the mathematical model of the SynRM and a short review of the DTC and DTC-SVM scheme based on [1], [16]. Finally, the control methods are evaluated in Matlab/Simulink and compared to FOC analyzing the phase current THD, torque ripple and torque transients of the SynRM.

## II. MOTOR EQUATIONS OF THE SYNRM

The voltage equations of the simulated machine model are defined in the rotor oriented reference frame as [16]:

$$v_q = Ri_q + L_q \frac{di_q}{dt} + \omega_e \lambda_d \quad (1)$$

$$v_d = Ri_d + L_d \frac{di_d}{dt} - \omega_e \lambda_q \quad (2)$$

$$\lambda_q = L_q i_q \quad (3)$$

$$\lambda_d = L_d i_d \quad (4)$$

where  $v_d, v_q$ : stator phase voltage;  $R$ : stator resistance;  $i_d, i_q$ : phase current;  $\omega_e$ : electrical rotor speed;  $L_d, L_q$ : stator phase inductance;  $\lambda_d, \lambda_q$ : stator flux-linkage.

The electromagnetic torque  $T_e$  is given for the three phase SynRM in the stator reference frame by [16]:

$$T_e = \frac{3p}{2} (\lambda_\alpha i_\beta - \lambda_\beta i_\alpha) \quad (5)$$

$$J \frac{d\omega_r}{dt} = T_e - T_l \quad (6)$$

where  $T_l$ : load torque;  $p$ : number of poles;  $J$ : motor inertia;  $\omega_r$ : mechanical rotor speed.

## III. CONTROL PRINCIPLES

### A. Direct Torque Control

The general DTC involves direct control of the stator flux-linkage and electromagnetic torque by applying optimal voltage switching vectors through the VSI. The DTC architecture as illustrated in Fig. 1 includes the estimation of the stator flux-linkage vector and its position and the electromagnetic torque estimation. The input of the bi-positional hysteresis comparators is the electromagnetic torque error and stator flux-linkage error.

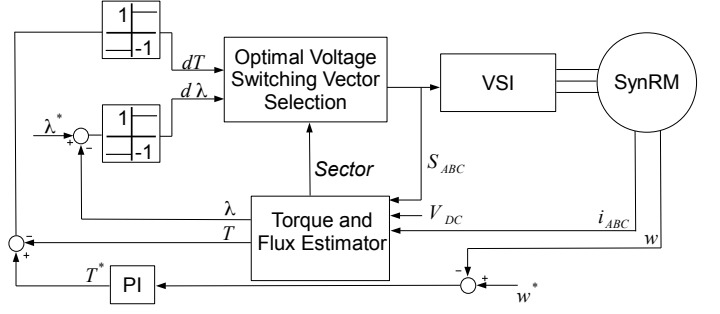


Fig. 1. Basic DTC Scheme

The reference torque is computed by the output of the speed controller and the reference flux-linkage modulus is given by the selected current angle control method as stated in [13] in dependence of the electromagnetic torque reference in accordance to (11). The selection of optimal VSI voltage vectors given in Table I depends on the output state  $d_\lambda$  and  $d_T$  of the bi-positional hysteresis comparator and the information of the stator flux-linkage sector position of  $\rho_{1-6}$  [16]. The stator flux-linkage vector  $\bar{\lambda}$  can be estimated from the stator voltage vector  $\bar{v}$  and stator current vector  $\bar{i}$  in the stationary reference frame by:

$$\bar{\lambda} = \int (\bar{v} - R\bar{i}) dt \quad (7)$$

An electromagnetic torque estimation can be computed through (5). The estimation of the stator phase voltages is obtained by the information of the VSI switching states using:

$$V_a = \frac{1}{3} V_{DC} (2S_A - S_B - S_C) \quad (8)$$

$$V_b = \frac{1}{3} V_{DC} (2S_B - S_A - S_C) \quad (9)$$

$$V_c = \frac{1}{3} V_{DC} (2S_C - S_A - S_B) \quad (10)$$

with  $S_{A,B,C} \{0, 1\}$  as the VSI gate signals for leg  $A, B, C$  (1 for upper switch on, lower switch off and 0 for upper switch off, lower switch on);  $V_{DC}$ : DC-Link voltage;  $V_{a,b,c}$ : stator phase voltage [16].

TABLE I. OPTIMUM ACTIVE SWITCHING VOLTAGE VECTOR LOOK-UP TABLE:  $\bar{v}_{1-6}(S_A, S_B, S_C)$ ;  $\bar{v}_1(1, 0, 0)$ ,  $\bar{v}_2(1, 1, 0)$ ,  $\bar{v}_3(0, 1, 0)$ ,  $\bar{v}_4(0, 1, 1)$ ,  $\bar{v}_5(0, 0, 1)$ ,  $\bar{v}_6(1, 0, 1)$  [16]

| $d_\lambda$ | $d_T$ | $p_1$       | $p_2$       | $p_3$       | $p_4$       | $p_5$       | $p_6$       |
|-------------|-------|-------------|-------------|-------------|-------------|-------------|-------------|
| 1           | 1     | $\bar{v}_2$ | $\bar{v}_3$ | $\bar{v}_4$ | $\bar{v}_5$ | $\bar{v}_6$ | $\bar{v}_1$ |
|             | -1    | $\bar{v}_6$ | $\bar{v}_1$ | $\bar{v}_2$ | $\bar{v}_3$ | $\bar{v}_4$ | $\bar{v}_5$ |
| -1          | 1     | $\bar{v}_3$ | $\bar{v}_4$ | $\bar{v}_5$ | $\bar{v}_6$ | $\bar{v}_1$ | $\bar{v}_2$ |
|             | -1    | $\bar{v}_5$ | $\bar{v}_6$ | $\bar{v}_1$ | $\bar{v}_2$ | $\bar{v}_3$ | $\bar{v}_4$ |

## B. Direct Torque Control - Space Vector Modulation

The general DTC scheme can be extended with SVM to obtain constant switching frequency and to reduce the stator phase current distortion [2], [8], [18]. A direct torque control method in stator reference frame for the PMSM is proposed in [1]. There, the stator voltage vector reference is predicted from an estimation of the stator flux-linkage vector with a displacement angle  $\Delta\delta$ . The electromagnetic torque  $T_e$  of the SynRM as a function of  $\delta$  is given by (11), (12), (13).

$$T_e = \frac{3p}{2} \left( \frac{1}{L_q} - \frac{1}{L_d} \right) \lambda^2 \frac{\sin(2\delta)}{2} \quad (11)$$

$$\lambda^2 = \lambda_d^2 + \lambda_q^2 \quad (12)$$

$$\rho = \theta + \delta = \theta + \tan^{-1} \frac{\lambda_q}{\lambda_d} = \tan^{-1} \frac{\lambda_\beta}{\lambda_\alpha} \quad (13)$$

where  $\lambda$  is the stator flux-linkage modulus and  $\delta$  is the angle of the stator flux-linkage space vector with position  $\rho$  with respect to the direct-axis of the rotor with position  $\theta$  as illustrated in Fig. 2 and described by (13) [16].

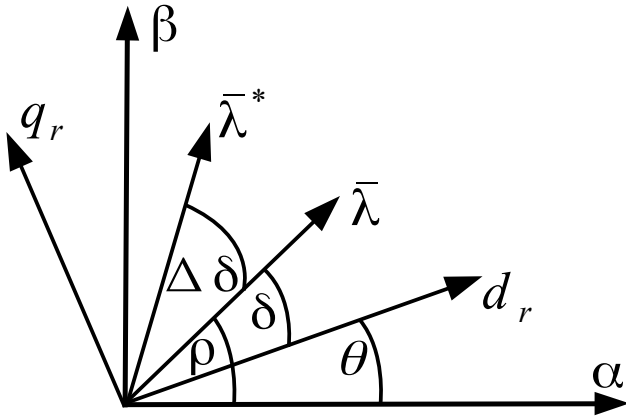


Fig. 2. Stator Flux-Linkage Phasor in the Stationary and Rotor Reference Frame

Reference [1] assumes a predictable torque error for a given stator flux-linkage reference  $\lambda^*$  which is shifted by an angle  $\Delta\delta$  with respect to  $\bar{\lambda}$ . In case of the SynRM the resulting torque error can be written as:

$$\Delta T_e = \frac{3p}{2} \left( \frac{1}{L_q} - \frac{1}{L_d} \right) \frac{1}{2} \left[ \lambda^{*2} \sin(2\delta + \Delta\delta) - \lambda^2 \sin(2\delta) \right] \quad (14)$$

The compensation of the torque error is achieved by considering the displacement angle  $\Delta\delta$  when the stator reference flux is predicted [1]. This is accomplished

by firstly writing (7) in discrete form with  $\Delta t$  as the sampling time as shown in (15), (16)

$$\lambda_\alpha(k) = [v_\alpha(k) - Ri_\alpha(k)] \Delta t + \lambda_\alpha(k-1) \quad (15)$$

$$\lambda_\beta(k) = [v_\beta(k) - Ri_\beta(k)] \Delta t + \lambda_\beta(k-1) \quad (16)$$

and by considering  $\Delta\delta$  in the flux-linkage prediction (17), (18).

$$\lambda_\alpha^*(k) = |\lambda^*(k)| \cos[\rho(k) + \Delta\delta(k)] \quad (17)$$

$$\lambda_\beta^*(k) = |\lambda^*(k)| \sin[\rho(k) + \Delta\delta(k)] \quad (18)$$

Finally, the stator reference voltages can be written as shown in (19), (20) [1], [2].

$$v_\alpha^*(k) = \frac{\lambda_\alpha^*(k) - |\lambda(k)| \cos \rho(k)}{\Delta t} + Ri_\alpha(k) \quad (19)$$

$$v_\beta^*(k) = \frac{\lambda_\beta^*(k) - |\lambda(k)| \sin \rho(k)}{\Delta t} + Ri_\beta(k) \quad (20)$$

The block diagram of the DTC-SVM architecture is shown in Fig. 3. The output of the torque controller functioned as the load displacement angle input of the space vector prediction stage. The reference modulus of the stator flux-linkage vector selection follows the current angle control method as stated in [13] in dependence of the electromagnetic torque reference in accordance to (11).

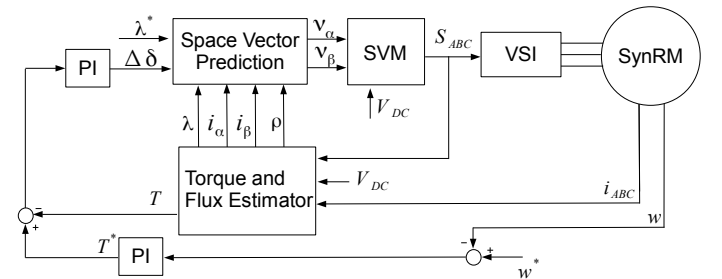


Fig. 3. DTC-SVM Scheme

## IV. SIMULATION RESULTS AND DISCUSSION

The following results are based on simulations in Matlab/Simulink. The DTC, DTC-SVM and FOC schemes are performed on the aforementioned model of the SynRM with parameters given in Table II. The machine model does not include saturation or cross coupling effects and iron- and friction losses are neglected. All simulation results are recorded at fixed base speed of the motor. For a fair comparison between DTC and

FOC/DTC-SVM, the flux and torque tolerance band of the bi-positional hysteresis comparators of the DTC are adjusted to perform at the same switching frequency as shown in Table III. The current angle of the control methods is adjusted to perform at maximum power factor (MPFC) in accordance to [13].

Figure 4 shows the phase current THD (Total Harmonic Distortion) as a function of the switching frequency. With increasing frequency all control methods result in reduced phase current distortion. The FOC and DTC-SVM result in similar current distortions which are lower than the distortion of the DTC scheme. Figure 4 also demonstrates that the SVM could be effectively adopted as DTC strategy for the SynRM in order to reduce the phase current distortion.

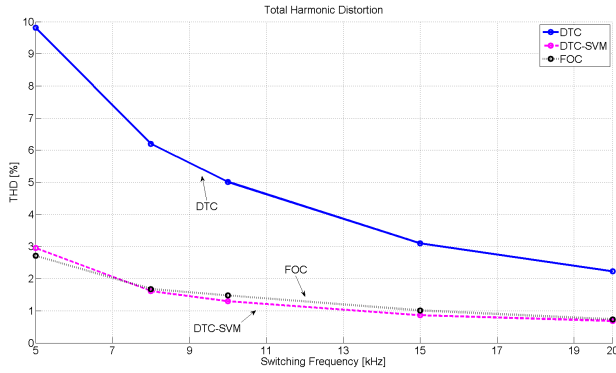


Fig. 4. Phase Current Distortion (THD) vs. Switching Frequency at fixed 220 rad/sec and 50Nm

The fast torque dynamic of the DTC and DTC-SVM is illustrated in Fig. 5. DTC and DTC-SVM reject the load disturbance step change faster compared to the FOC, whereby DTC-SVM displays larger undershoot. The resulting torque ripple of the DTC is significant higher compared to FOC and DTC-SVM which is also illustrated in Fig. 6 over various switching frequencies. The lowest torque ripple achieves the DTC-SVM scheme at each measured operation point. The current THD and the torque distortion of the DTC scheme increase faster for decreasing frequency in comparison to the DTC-SVM and FOC.

TABLE II. SYNRM PARAMETER

|                          |                             |
|--------------------------|-----------------------------|
| DC-Bus Voltage           | $V_{DC} = 800V$             |
| Stator Resistance        | $R = 0.1518\Omega$          |
| D-Axis Stator Inductance | $L_d = 0.035H$              |
| Q-Axis Stator Inductance | $L_q = 0.003H$              |
| Motor Inertia            | $J = 0.0688kg^2$            |
| Number of Poles          | $p = 4$                     |
| Full Load                | $T_l = 100Nm$               |
| Base Speed               | $w_r = 220 \frac{rad}{sec}$ |

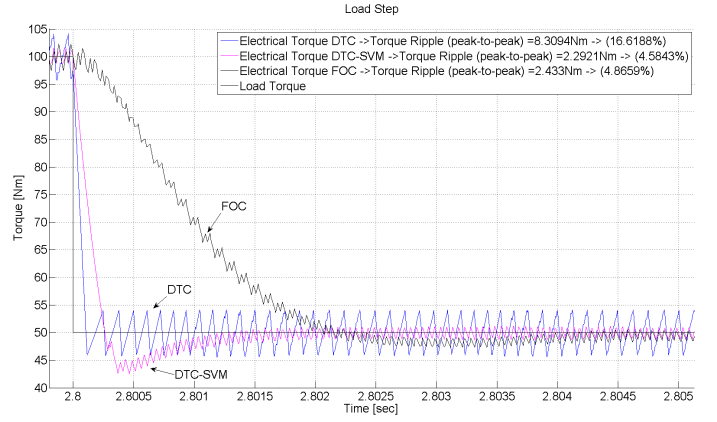


Fig. 5. Load Step 100Nm to 50 Nm at fixed 220 rad/sec and 10 kHz

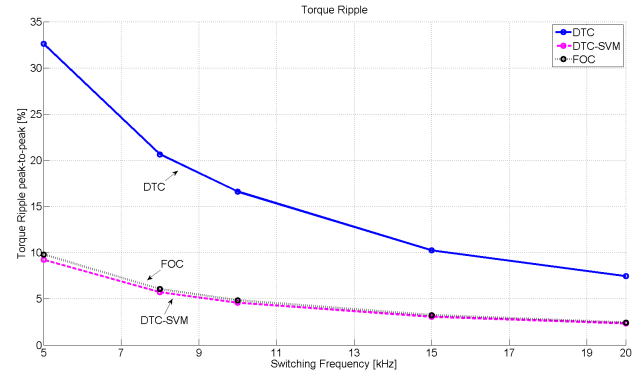


Fig. 6. Torque Ripple vs. Switching Frequency at fixed 220 rad/sec and 50Nm

TABLE III. DTC TOLERANCE BAND PARAMETERS AT DIFFERENT FREQUENCIES

| f [kHz]                              | 5     | 8     | 10    | 15    | 20    |
|--------------------------------------|-------|-------|-------|-------|-------|
| $\Delta T [Nm]$ (peak to peak)       | 16    | 10    | 8     | 4.4   | 3.4   |
| $\Delta \lambda [Wb]$ (peak to peak) | 0.001 | 0.001 | 0.001 | 0.001 | 0.001 |

## V. CONCLUSION

This paper presented a comparative evaluation of DTC, DTC-SVM and FOC strategies with respect to phase current and torque distortion at different switching frequencies. It has been shown that DTC of the SynRM can be extended with SVM in the stator reference frame by using a prediction of the stator flux-linkage in consideration of a flux-linkage displacement angle. The DTC-SVM results in most of the measured cases in reduced phase current distortion and reduced torque ripples at various switching frequencies compared to the general DTC and FOC and achieved faster reference torque tracking in comparison to FOC. For this reason, DTC-SVM can be considered as an adequate alternative to the general FOC and DTC in SynRM applications where high dynamic torque disturbances must be compensated within a minimum amount of time.

## ACKNOWLEDGMENT

This paper is part of the ADvanced Electric Powertrain Technology (ADEPT) project which is an EU funded Marie Curie ITN project, grant number 607361. Within ADEPT a virtual and hardware tool are created to assist the design and analysis of future electric propulsions. Especially within the context of the paradigm shift from fuel powered combustion engines to alternative energy sources (e.g. fuel cells, solar cells, and batteries) in vehicles like motorbikes, cars, trucks, boats, planes. The design of these high performance, low cost and clean propulsion systems has stipulated an international cooperation of multiple disciplines such as physics, mathematics, electrical engineering, mechanical engineering and specialisms like control engineering and safety. By cooperation of these disciplines in a structured way, the ADEPT program provides a virtual research lab community from labs of European universities and industries [22].

## REFERENCES

- [1] M. Fu and L. Xu, *Sensorless Direct Torque Control Technique for Permanent Magnet Synchronous Motors*, IEEE, Industrial Applications Conference, Vol. 1, pp. 159-164, 1999.
- [2] D. Swierczynski and M. Kazmierkowsky and F. Blaabjerg, *DSP Based Direct Torque Control of Permanent Magnet Synchronous Motor (PMSM) Using Space Vector Modulation (DTC-SVM)*, IEEE, Industrial Electronics, Vol. 3, pp. 723-727, 2002.
- [3] W. Leonhard, *Field-Oriented for controlling AC-Machines Principle and Application*, IEEE, Power Electronics and Variable-Speed Drives, pp. 277-282, 1988.
- [4] A. Kilthau and J. M. Pacas, *Parameter-Measurement and Control of the Synchronous Reluctance Machine including Cross Saturation*, IEEE, Industry Applications Conference, Vol. 4, pp. 2302-2309, 2001.
- [5] D. Casadei and F. Profumo and G. Serra and A. Tani, *FOC and DTC: Two Variable Schemes for Induction Motors Torque Control*, IEEE Transactions on Power Electronics, Vol. 17, No. 5, 2002.
- [6] A. Kadir and S. Mekhilef and W. Hew, *Comparison of Basic Direct Torque Control Designs for Permanent Magnet Synchronous Motor*, 7th International Conference on Power Electronics and Drive Systems (PEDS), pp. 1344-1349, 2007.
- [7] X.T.Garcia and B. Zigmund and A. Terlizzi and R.Pavlanin and L. Salvatore, *Comparison between FOC and DTC strategies for permanent magnet synchronous motor*, Advances in Electrical and Electronics Engineering, 2006.
- [8] C. Lascu and I. Boldea and F. Blaabjerg, *A Modified Direct Torque Control for Induction Motor Sensorless Drive*, IEEE Transactions on Industrial Applications, Vol. 36, No.1, 2000.
- [9] S. Kang and S. Sul, *Highly Dynamic Torque Control of Synchronous Reluctance Motor*, IEEE Power Electronics Specialists Conference, Vol. 2, pp. 1793-1797, 1996.
- [10] L. Xu and X. Xu and T. A. Lipo and D. W. Novotny, *Vector Control of a Synchronous Reluctance Motor Including Saturation and Iron Loss*, IEEE Transaction on Industrial Applications, Vol. 27, No. 5, 1991.
- [11] A. Chiba and T. Fukao, *A Closed-Loop Operation of Super High-Speed Reluctance Motor for Quick Torque Response*, IEEE Transactions on Industry Applications, Vol. 28, No. 3, 1992.
- [12] A. Vagati, *The Synchronous Reluctance Solution: A new alternative in A.C. Drives*, IEEE Industrial Electronics, Control and Instrumentation, Vol. 1, pp. 1-13, 1994.
- [13] R.E. Betz and M. Jovanovic and R. Lagerquist and T.J.E. Miller, *Aspects of the Control of Synchronous Reluctance Machine Including Saturation and Iron Losses*, IEEE, Industry Applications Society Annual Meeting, Vol. 1, pp. 456-463, 1992.
- [14] A. Consoli and G. Scarcell and A. Testa, *Self Synchronizing Torque Control of Reluctance Motor Drives*, IEEE, Power Electronics Specialists Conference, Vol. 1, pp. 344-350, 1996.
- [15] T.J.E. Miller and A. Hutton and C. Cossar and D. A. Staton, *Design of a Synchronous Reluctance Motor Drive*, IEEE, Transaction on Industrial Applications, Vol. 27, No. 4, 1991.
- [16] P. Vas, *Sensorless Vector and Direct Torque Control*, Oxford University Press, 1998.
- [17] F. Niu and K.Li and B. Wang and E. G. Strangas, *Comparative Evaluation of Direct Torque Control Strategies for Permanent Magnet Synchronous Machines*, IEEE, Applied power Electronics Conference and Exposition, pp. 2438-2445, 2014.
- [18] I. Boldea and L. Janosi and F. Blaabjerg, *A Modified Direct Torque Control (DTC) of Reluctance Synchronous Motor Sensorless Drive*, Electric Machines and Power Systems, Vol. 28, 2000.
- [19] R. R. Moghaddam and F. Magnussen and C. Sadarangani, *Theoretical and Experimental Reevaluation of Synchronous Reluctance Machine*, Industrial Electronics, Vol. 57, pp. 6-13, 2010.
- [20] P. Matyska, *Advantages of Synchronous Reluctance Machine*, Transactions on Electrical Engineering, Vol. 3, No. 2, 2014.
- [21] A. Tammi and R. R. Moghaddam and L. R. Thand, *ABB Review 1/2011*, Technical Report, ABB, 2011.
- [22] A. Stefanskyi and A. Dziechciarz and F. Chauvicourt and G. E. Sfakianakis and K. Ramakrishnan and K. Niyomsatian and M. Curti and N. Djukic and P. Romanazzi and S. Ayat and S. Wiedemann and W. Peng and S. Stipetic, *Researchers within the EU funded Marie Curie ITN project ADEPT, grant number 607361*, 2013-2017.